

ELECTRON TRANSMISSION THROUGH THICK SILICON TARGETS

By Jag J. Singh

Langley Research Center
Langley Station, Hampton, Va.

NATIONAL AERONAUTICS AND SPACE ADMINISTRATION

For sale by the Clearinghouse for Federal Scientific and Technical Information
Springfield, Virginia 22151 - CFSTI price \$3.00

ELECTRON TRANSMISSION THROUGH THICK SILICON TARGETS

By Jag J. Singh
Langley Research Center

SUMMARY

Results of some recent measurements on angular and energy distribution of fast electrons transmitted through silicon targets of thicknesses varying from about 10 percent to 50 percent of the mean range are compared with theoretical calculations based on the Goudsmit-Saunderson treatment of multiple coulomb scattering of electrons. Effects of fluctuations of collision losses of the incident electrons have been included in the theory. It is concluded that the presently available theoretical calculations predict a somewhat lower value of the width of the transmitted electron spectra than measurements indicate.

INTRODUCTION

Proper evaluation of the electron hazard in space requires an accurate knowledge of the electron-diffusion process in material targets. A large number of theoretical studies (e.g., refs. 1 to 8) have dealt with the penetration of charged particles in material media. However, an exact theoretical treatment of this problem is extremely complex and does not lend itself conveniently to practical applications. Consequently, most of the theoretical studies involve some form of approximation and are usually limited in their domain of applicability. In view of these difficulties, it is necessary to make an experimental evaluation of the multiple-scattering process in order to make reliable predictions needed for such applications as space-shielding design and radiation-damage studies.

The immediate objective of the present investigation was to test a computer program dealing with the diffusion of electrons in matter. Such a program, based on a combination of diffusion-type Goudsmit-Saunderson theory (refs. 1 and 2) with Monte-Carlo random-sampling technique, had been written in connection with thick-target electron-bremsstrahlung measurements recently completed at this laboratory.

SYMBOLS

E_{incident} energy of incident electron

G_l total average of Legendre polynomial of the order l

n	number of collisions suffered by an electron
$I(\theta)$	intensity at angle θ
$P(\theta)d\theta$	probability that the scattering angle lies between θ and $\theta + d\theta$
$P_l(\cos \theta)$	Legendre polynomial of the order l
$W(n)$	probability that n scattering events occurred
$W(\theta)$	angular distribution function
θ	angle between the direction of the incident electron and the transmitted electrons observed

Notations:

FWHM	full width at half maximum height
Si(Li)	lithium-drift silicon detector

EXPERIMENTAL PROCEDURE

Electrons of energies 1.00, 1.50, and 2.00 MeV from an electrostatic generator were allowed to fall normally on 2-centimeter-diameter silicon targets of thickness ranging from 10 percent to 50 percent of the effective electron range in silicon. The choice of silicon targets was suggested by the widespread use of silicon devices in space missions. The beam size on the target was restricted to a 2-millimeter-diameter spot with the help of a focussing magnet and a series of aluminum collimators. Adequate lead shielding was provided to stop most of the bremsstrahlung produced at the collimators and along the beam tube. Transmitted electron spectra were measured at various angles between 15° and 150° with 5-millimeter-deep lithium-drift silicon detectors. Figure 1 is a schematic diagram of the experimental setup. A triple collimator assembly, of the type shown in figure 2, was mounted in front of each detector to reduce the angular spread of the electrons arriving at the detector face to less than 1° . This assembly also reduced the number of electrons arriving at the detector after scattering from the target chamber walls. The detectors were calibrated by using a 1-microcurie bismuth 207 radioactive source. Figure 3 shows a typical calibration spectrum. The precise incident electron energy in the case of 1-MeV experiment was measured by observing

electrons elastically scattered from a $100\text{-}\mu\text{g}/\text{cm}^2$ -thick gold target (gold spectra). At 1.50 MeV and 2.00 MeV, the information about electron energy was obtained by using a calibrated analyzing magnet as well as a calibrated Si(Li) detector. Gold spectra were taken at the beginning and end of the series of runs for each target thickness. These spectra provided a quantitative measure of the beam energy shift or the electronics gain shift during the runs. Such a shift was found to be less than 1 percent per 24 hours. Figures 4 and 5 show typical gold spectra observed at 1.00 MeV and 1.50 MeV. From these spectra, it is obvious that the beam energy resolution – including the effects of finite resolution of the detectors and incident electron energy inhomogeneity – is approximately 50 keV (FWHM). The incident electron charge was monitored with another lithium-drift detector located at 75° to the beam direction. This monitor counter was biased to reject all particles with energies equal to or less than 600 keV. This discrimination level insured that the major portion of the bremsstrahlung produced at the target and the detector collimators was not allowed to reach the monitor electronics. In the case of measurements at 1.50 MeV and 2.00 MeV, the total incident charge on the target was also monitored by using a shallow ionization chamber between the target chamber and the analyzing magnet. Measurements were made at each angle with and without a 5-millimeter-thick aluminum disk in front of the movable counter. With the absorber disk in place, the detector could only "see" the background X-rays.

The output of the movable detector, after suitable pulse shaping and amplification, was fed into a 400-channel pulse-height analyzer. The incident electron beam was adjusted so that the dead-time correction to the pulse-height analyzer was less than 10 percent at all angles.

EXPERIMENTAL RESULTS

Before the experimental data can be compared with the theory, it is essential to take into account the finite resolving power of the lithium-drift detectors for monoenergetic electrons. The experimental data could be corrected or the theoretical results could be modified to allow for the finite resolving power of the detectors. The latter approach was considered more convenient and was used in this investigation. (See appendix for details.) It has been assumed that, in the detection system used, 1- to 2-MeV electrons produce Gaussian peaks with full width at half maximum height (FWHM) of 50 keV. This assumption is not strictly justifiable in view of the low-energy tail associated with the main Gaussian peak as seen in figures 4 and 5. However, this simplification is not expected to introduce large errors.

Transmission electron spectra for normal incidence, after subtracting appropriate background, have been obtained at various angles for each target thickness at the three

incident electron energies. The details of these data are discussed in the following paragraphs. (See ref. 9 for measurements at 1.00 MeV.)

Energy Distribution of Transmitted Electrons

The typical experimental energy spectra of the transmitted electrons along with the calculated spectra are shown in figures 6 to 9. For proper comparison, the two spectra have been normalized to have equal intensities at their respective peaks.

Angular Distribution of Transmitted Electrons

The measured angular distribution (number) of the transmitted electrons along with the calculated functions are shown in figures 10 to 12. The experimental intensities used in these figures include only the electrons within the spectral limits predicted by the theory. The measured and calculated angular-distribution functions have been normalized to have equal peak amplitudes for the convenience of comparison.

COMPARISON WITH THEORY

Electrons traveling through material media of finite thickness suffer a very large number of scatterings. These single deflections combine statistically to give a sort of modified normal error curve about an average deflection. The first general theory of multiple scattering along these lines was developed by Williams (refs. 7 and 8). According to this theory, the statistical angular-distribution function after many scatterings is given by the Gaussian distribution function of the form:

$$P(\theta)d\theta = \frac{2\theta}{\theta^2} \exp\left(-\frac{\theta^2}{\theta^2}\right)d\theta$$

where $P(\theta)d\theta$ is the probability of deflection lying between

$$\theta \quad \text{and} \quad \theta + d\theta$$

and $\overline{\theta^2}$ is the mean squared scattering angle. This theory, however, is incomplete as it says nothing about plural scattering – a case where more than one deflection occurs while not enough scatterings are involved to give characteristic Gaussian distribution. Recently Goudsmit-Saunderson (refs. 1 and 2), Molière (refs. 4 to 6), and Snyder-Scott (ref. 3) have given a detailed treatment of the basic multiple-scattering theory. The two most useful theories appear to be the Goudsmit-Saunderson theory for thick targets and the Molière theory for small angles and thin targets. The Goudsmit-Saunderson theory, which is used in this report, makes use of the geometrical property of the Legendre

polynomials that the average value of any polynomial after n impacts is equal to the n th power of the average value of the polynomial after one impact, provided that the law of scattering is cylindrically symmetrical, that is,

$$\langle P_l(\cos \theta) \rangle = \left[\langle P_l(\cos \theta_1) \rangle \right]^n$$

The final total average of any Legendre polynomial will be the average considering all possible values of n , where n is the number of collisions suffered by the electron. Denoting the average value by G_l and the probability that an electron makes n collisions by $W(n)$, one gets

$$G_l = \sum_0^{\infty} W(n) \left[\langle P_l(\cos \theta_1) \rangle \right]^n$$

These average values of G_l completely determine the angular distribution of the emerging electrons. The Goudsmit-Saunderson theory holds for all angles of deflection and is exact if one considers the electrons with the same total path length in the scatterer. This theory, including the effects of energy loss and in combination with the Monte-Carlo technique, has been applied to the electron-transport problem by Berger (refs. 10 and 11).

In reference 9 the predictions of the Goudsmit-Saunderson theory, in the continuous slowing-down approximation, were compared with the experimental results. The experimental energy and angular distributions were much broader than the theoretical distributions. In the present report, the experimental results have been compared with the Monte-Carlo calculations of Berger (refs. 10 and 11). The effects of fluctuations in the ionization energy loss are included but no account has been taken of the fluctuations in the bremsstrahlung loss and secondary knock-on electrons in these calculations. The theoretical results are based on a sample of 16 000 histories generated by a program which kept the number of electrons penetrating to various slab thicknesses essentially the same but compensated for this by giving the electrons a suitable probability factor. The transmitted electrons were grouped into 25-keV energy bins and 5° angular cones. The computations were broken off at 100 keV. In the following pages, a detailed comparison between the experiment and the theory at 1.00 MeV is made, and the data at 1.50 MeV and 2.00 MeV are discussed in terms of the corresponding theoretical results at 1.00 MeV. This approach is justifiable because the shape of the transmission curve is quite insensitive to the value of the source energy, when expressed as a function of the ratio of target thickness to the mean range of the incident electrons (refs. 10 and 11). Thus, for

example, the shape of the calculated transmitted electron spectra at 1.00 MeV through a target whose thickness is 20 percent of the mean range of 1.00-MeV electrons is quite similar to the transmitted spectra at 1.50 MeV through a target whose thickness is 20 percent of the range of 1.50-MeV electrons.

Furthermore, theoretical Monte-Carlo calculations made for aluminum have been adapted for comparison with the experimental data in silicon since minor differences in multiple scattering and screening effects will have very small effects on calculations.

Energy Distribution

Figures 6 and 7 show the comparison between the Monte-Carlo calculations of Berger (refs. 10 and 11) and the experimental results at 1.00 MeV. Also shown in these figures are the theoretical calculations in the continuous slowing down approximation taken from reference 9. In the case of 1.50-MeV and 2.00-MeV results as shown in figures 8 and 9, the theoretical Monte-Carlo spectra were obtained from reference to the corresponding 1.00 MeV spectra. It is evident that the theory in the form used in this report underestimates the multiple-scattering effects especially in the region below the mean energy loss. Part of the low-energy experimental electron spectrum could be due to scattering at the collimator edges and the backscattering at the detector surface. But the fact that the disagreement between the theory and the experiment is a function of the target thickness points toward the need for a more accurate theoretical approach to the electron-transport problem.

Angular Distribution

Figure 10 shows the comparison between the Monte-Carlo calculations of Berger (refs. 10 and 11) and the experimental results on the angular distribution of the transmitted electrons for a number of target thicknesses at 1.00 MeV. Figures 11 and 12 show the comparison between theory and experiment at 1.50-MeV and 2.00-MeV electron energies. It appears that the experimental mean scattering angle is slightly larger than that predicted by the theory. This result is quite consistent with the data on the energy distribution. Figures 13 and 14 show comparison between the experimental data at different energies and a distribution function of the form:

$$W(\theta) = (a \cos \theta + b \cos^2 \theta) \sin \theta$$

Such a function appears as a leading term in the Bethe et al. (ref. 12) formalism where they disregard the electron energy loss. The experimental distributions are broader than the Bethe function. Furthermore, it should be noted that beyond a certain target thickness, the half-width of the experimental angular distribution remains constant as

noted by Frank (ref. 13). This point is illustrated in figure 15 where average cosine θ , $\langle \cos \theta \rangle$, defined as

$$\langle \cos \theta \rangle = \frac{\sum_i n_i \cos \theta_i}{\sum_i n_i}$$

is plotted against target thickness. A summary of these results is presented in table I.

CONCLUDING REMARKS

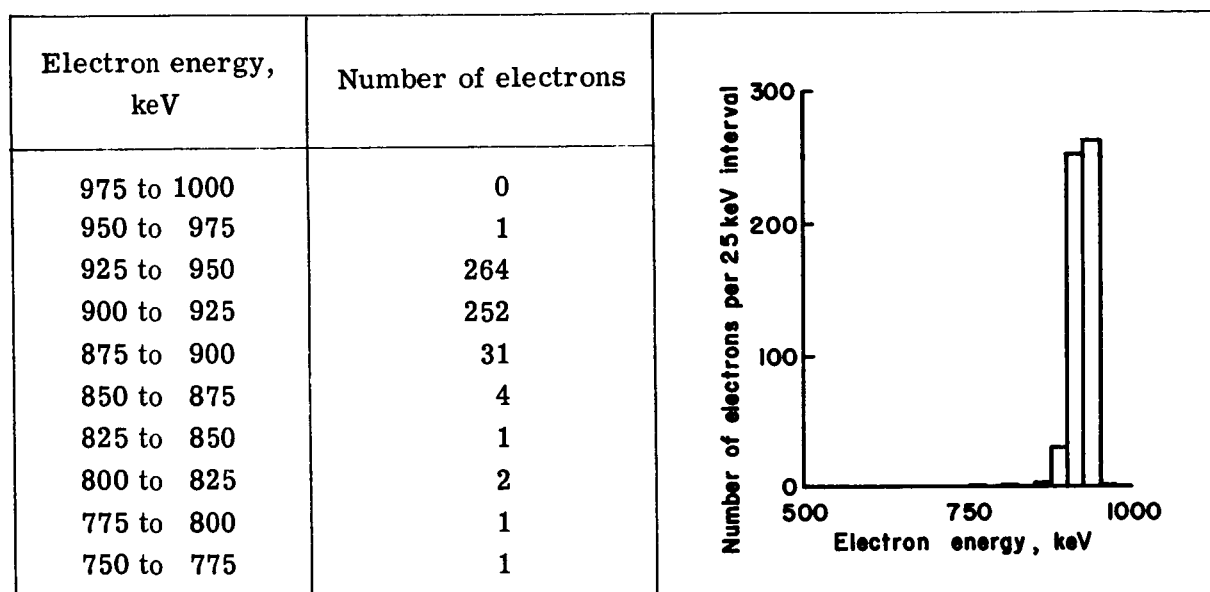
An investigation of electron transmission through thick silicon targets has shown that the measured spectra have a considerably greater width than the calculated spectra in the continuous slowing-down approximation. The inclusion of fluctuations in the electron ionization energy loss in the theoretical calculations, as done by Berger, leads to better agreement between the theory and the experiment. This agreement is mainly due to the fact that the energy-loss straggling allows both slower and faster electrons to emerge from the foils than would be possible in the continuous slowing-down approximation. As indicated earlier, the effects of the fluctuations of the radiation loss and the contribution from the secondary knock-on electrons have not been included in the theoretical calculations. Inclusion of these effects along with the use of more accurate detector-response functions to monoenergetic electrons is expected to bring the theory and the experiment into better agreement. Since the width of the transmission energy spectra is strongly dependent on the energy-loss straggling theory used in the Monte-Carlo calculations, the use of a more appropriate theory of energy-loss fluctuations is required.

Langley Research Center,
National Aeronautics and Space Administration,
Langley Station, Hampton, Va., October 28, 1966,
124-09-01-09-23.

APPENDIX

TECHNIQUE OF MODIFYING THE THEORETICAL ELECTRON TRANSMISSION HISTOGRAM TO INCLUDE THE EFFECTS OF FINITE RESOLVING POWER OF THE DETECTOR SYSTEM

Consider the case of transmission of 1-MeV electrons through a silicon target whose thickness corresponds to 10 percent of the mean range of 1-MeV electrons. Suppose the angle of observation ranges from 40° to 45° with respect to the normally incident electron-beam direction. The energy distribution of the transmitted electrons is given by the following histogram (see refs. 10 and 11):



For the sake of clarity, consider the effects of finite resolution of the detection system on the electrons of energy 925 to 950 keV. During the measurements, the electronic system gain was such that 25 keV covered six channels of the pulse-height analyzer. If it is assumed that the distribution of electrons over the region of 925 to 950 keV was uniform, each channel in that region would have 44 counts. (Strictly speaking, this is not correct and a better approach would have been to calculate the number of electrons in the energy regions whose widths corresponded to a single channel of the pulse-height analyzer. However, this approach would have resulted in an inordinately long computation time and is not expected to alter the shape of the energy spectrum any more than the statistical errors due to a finite number of electron histories.) Now consider the channel whose mean energy is 947.9 keV, that is, the channel at the high-energy end of the 925- to 950-keV energy region. Assuming a FWHM of 50 keV for monoenergetic

APPENDIX

electrons, a Gaussian peak with a half-width of 12 channels centered at 947.9 keV is drawn such that the total number of counts in all the channels covered by the Gaussian peak equals 44. This process is repeated for each of the remaining 5 channels in the 925- to 950-keV energy region. The six Gaussian peaks thus obtained are added to give a "compound" peak centered at 937.5 keV. This process is repeated for all the 25-keV regions listed above and the various "compound" peaks are added to give the theoretically calculated transmitted electron spectrum. It should be emphasized that the monoenergetic electrons do not produce exactly Gaussian peaks in the detection system used in the present investigation. There is always a small low-energy tail, due to backscattering at the detector, associated with the main Gaussian peak. However, the omission of the weak tail is not expected to make more than a few percent error in the lower energy part of the theoretical spectrum. In future measurements, it is planned to include the tail along with the main Gaussian peak in reducing the electron histograms to the form where a direct comparison with the experiment can be made.

REFERENCES

1. Goudsmit, S.; and Saunderson, J. L.: Multiple Scattering of Electrons. *Phys. Rev.*, Second ser., vol. 57, no. 1, Jan. 1, 1940, pp. 24-29.
2. Goudsmit, S.; and Saunderson, J. L.: Multiple Scattering of Electrons. II. *Phys. Rev.*, Second ser., vol. 58, no. 1, July 1, 1940, pp. 36-42.
3. Snyder, H. S.; and Scott, W. T.: Multiple Scattering of Fast Charged Particles. *Phys. Rev.*, Second ser., vol. 76, no. 2, July 15, 1949, pp. 220-225.
4. Molière, G.: Theory of Scattering of Fast Charged Particles. I. Single Scattering in a Screened Coulomb Field. *Z. Naturforsch.*, pt. a, vol. 2, Mar. 1947, pp. 133-145.
5. Molière, G.: Theory of Scattering of Fast Charged Particles. II. Plural and Multiple Scattering. *Z. Naturforsch.*, pt. a, vol. 3, Feb. 1948, pp. 78-97.
6. Molière, G.: Theory of Scattering of Fast Charged Particles. III. The Multiple Scattering From Tracks With Consideration of Statistical Coupling. *Z. Naturforsch.*, pt. a, vol. 10, no. 3, 1955, pp. 177-211.
7. Williams, E. J.: Concerning the Scattering of Fast Electrons and of Cosmic-Ray Particles. *Proc. Roy. Soc. (London)*, ser. A, vol. 169, no. 939, Mar. 7, 1939, pp. 531-572.
8. Williams, E. J.: Multiple Scattering of Fast Electrons and Alpha-Particles, and "Curvature" of Cloud Tracks Due to Scattering. *Phys. Rev.*, Second ser., vol. 58, no. 4, Aug. 15, 1940, pp. 292-306.
9. Singh, Jag J.: Transmission of Electrons Through Thin Silicon Foils. *Bull. Am. Phys. Soc.*, ser. 11, vol. 10, no. 1, Jan. 27, 1965, p. 68.
10. Berger, Martin J.: Monte Carlo Calculation of the Penetration and Diffusion of Fast Charged Particles. *Methods in Computational Physics, Vol. I - Statistical Physics*, Berni Alder, Sidney Fernbach, and Manuel Rotenberg, eds., Academic Press, 1963, pp. 135-215.
11. Berger, M. J.; and Seltzer, S. M.: Results of Some Recent Transport Calculations for Electrons and Bremsstrahlung. *Second Symposium on Protection Against Radiations in Space*, Arthur Reetz, Jr., ed., NASA SP-71, 1965, pp. 437-448.
12. Bethe, H. A.; Rose, M. E.; and Smith, L. P.: Multiple Scattering of Electrons. *Proc. Am. Phil. Soc.*, vol. 78, 1938, pp. 573-585.
13. Frank, H.: Multiple Scattering and Back-Diffusion of Fast Electrons After Passage Through Thick Layers. *Z. Naturforsch.*, pt. a, vol. 14, 1959, pp. 247-261.

TABLE I
SUMMARY OF RESULTS ON AVERAGE ANGLE OF DEFLECTION
OF ELECTRONS THROUGH SILICON

Electron energy, MeV	Target thickness, mm	$\langle \cos \theta \rangle$ (a)	Diffusion length, mm
1.00	0.25	0.8920	0.65 ± 0.10
	.50	.7800	
	.68	.7510	
	.75	.7500	
1.50	.24	.8461	1.20 ± 0.10
	.53	.7609	
	.78	.7279	
	1.05	.7452	
	1.27	.7440	
	1.52	.7468	
2.00	.32	.9401	1.90 ± 0.20
	.76	.7497	
	.97	.7849	
	1.27	.7151	
	1.52	.7600	
	1.95	.7500	

^aThe errors on $\langle \cos \theta \rangle$ are of the order of 10 percent.

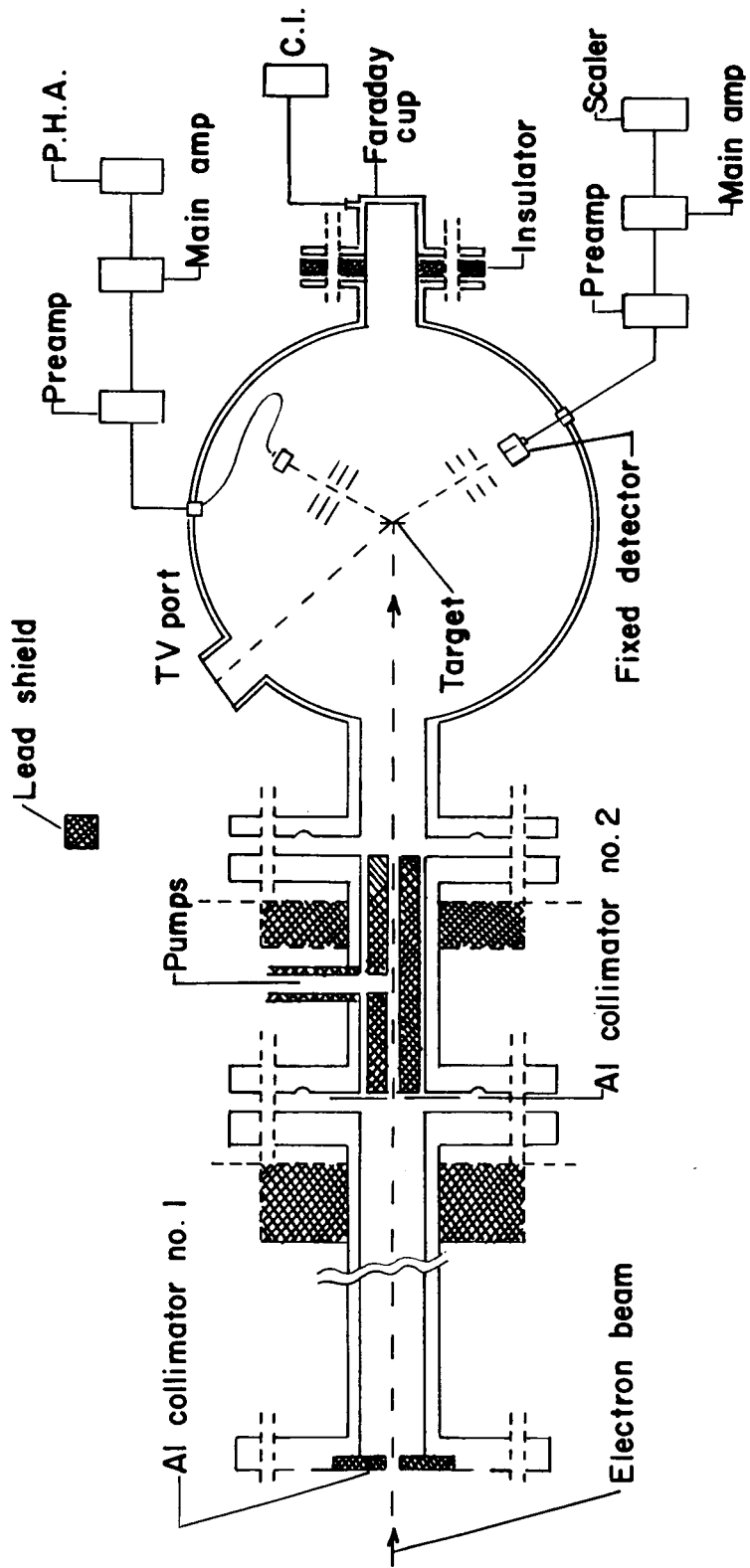


Figure 1.- Schematic diagram of general experimental setup.

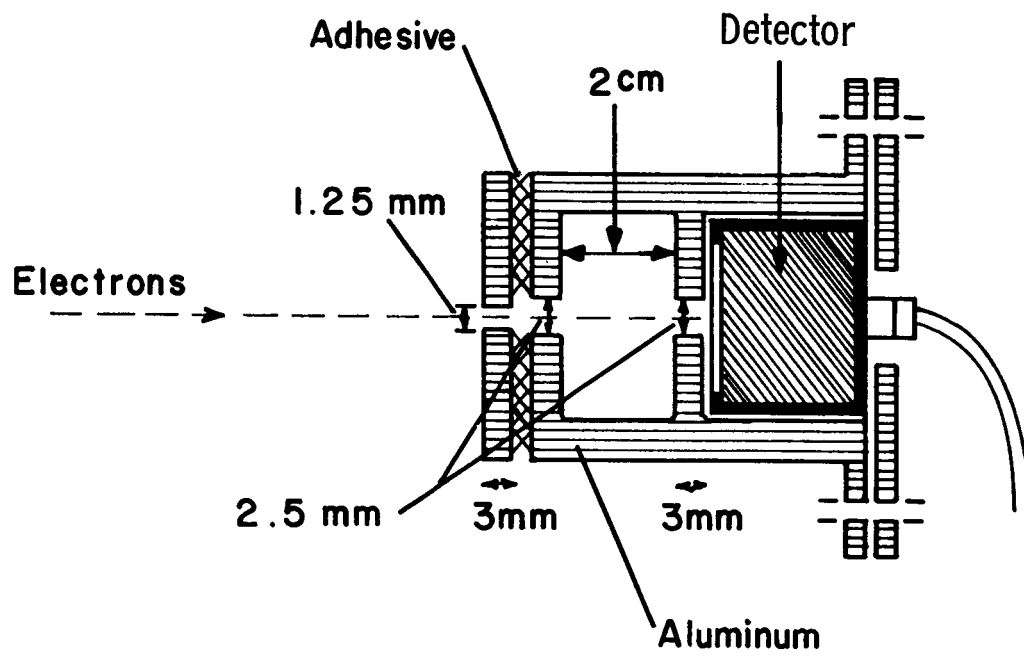


Figure 2.- Details of antiscatter collimator assembly.

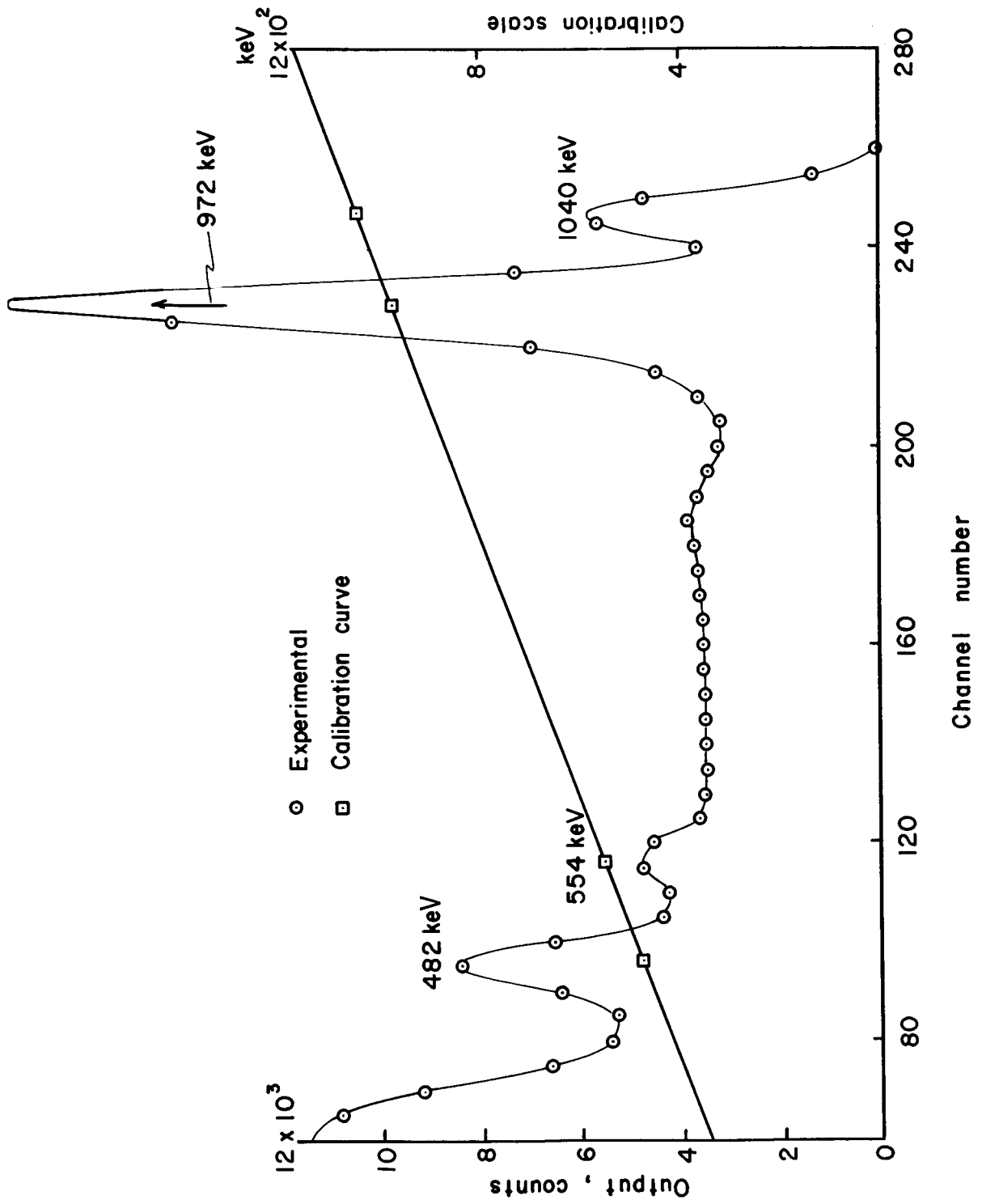


Figure 3.- Bismuth 207 calibration spectrum.

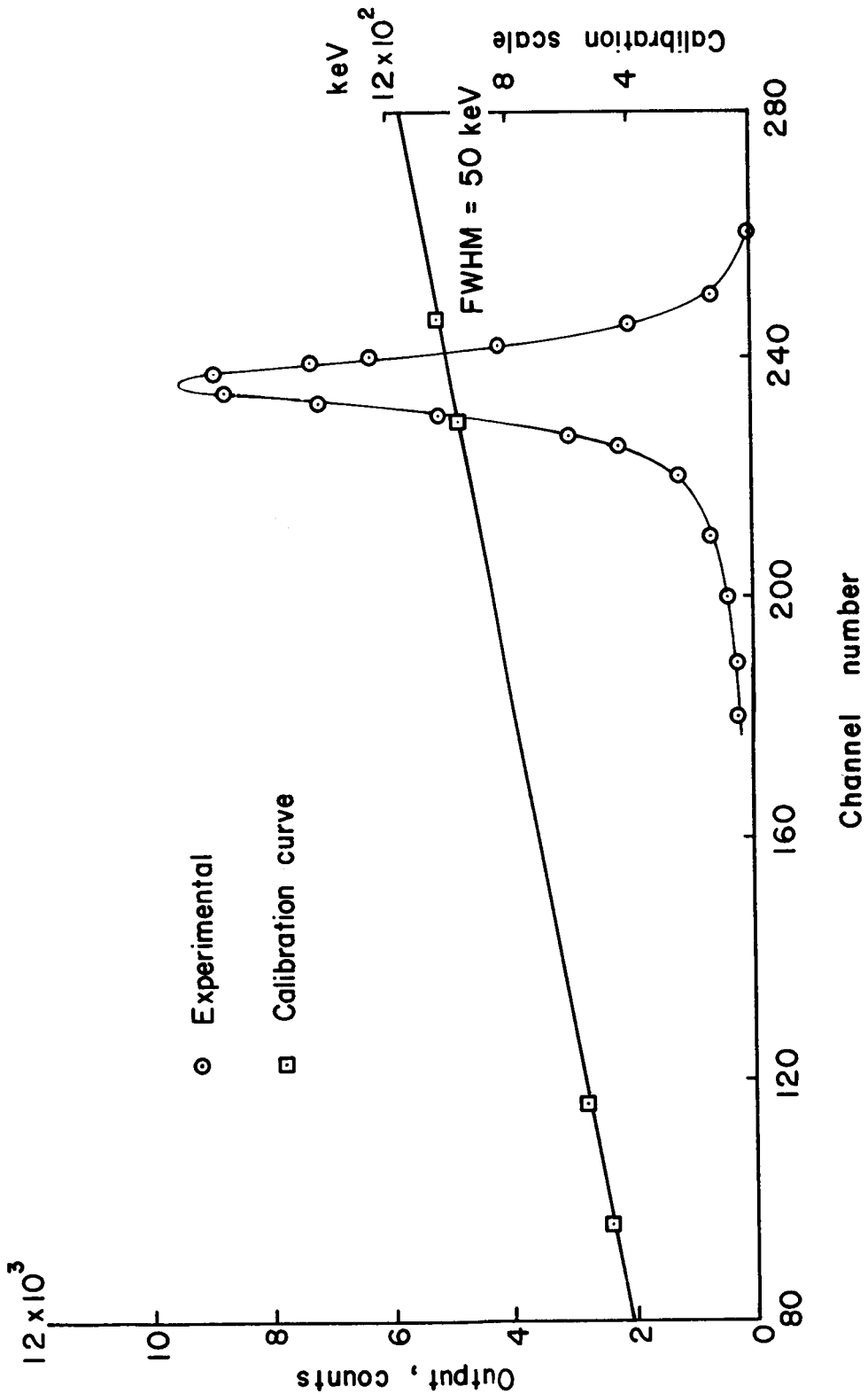


Figure 4.- Spectrum of 1.00-MeV electrons elastically scattered from thin gold foil.

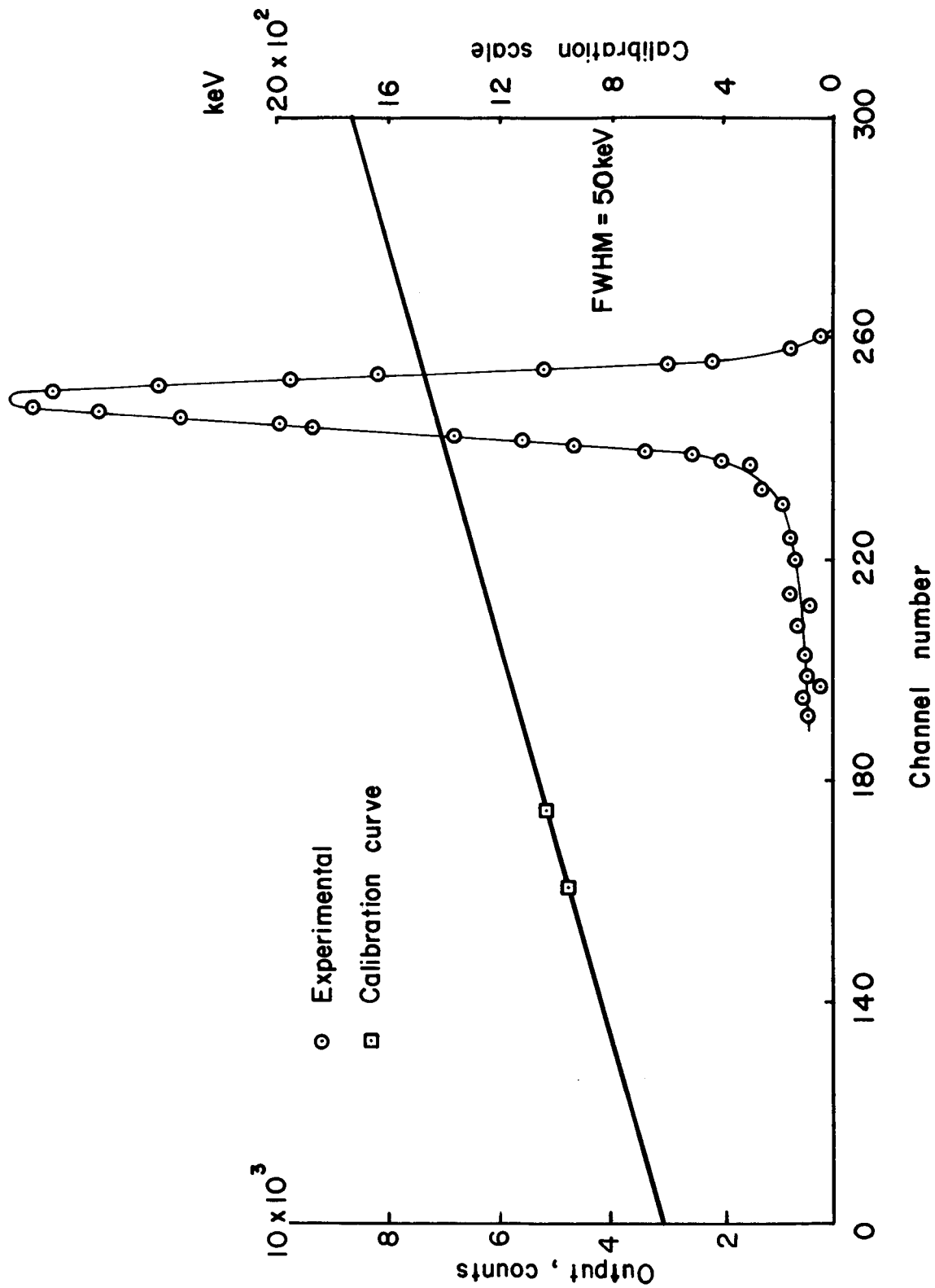


Figure 5.- Spectrum of 1.50-MeV electrons elastically scattered from thin gold foil.

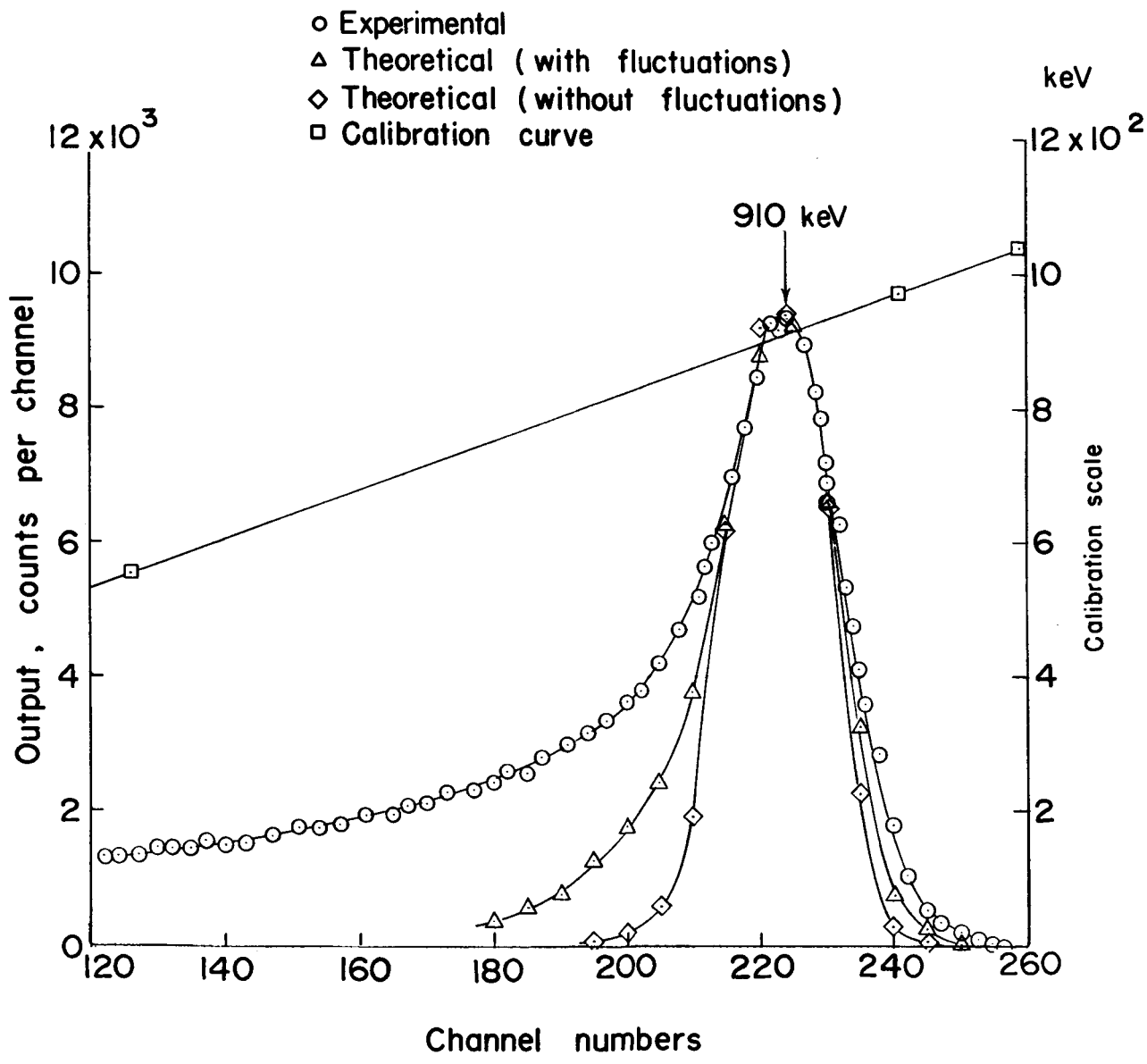


Figure 6.- Comparison between theory and experimental spectrum of 1.00-MeV electrons transmitted through 0.25-mm-thick silicon target at 45°.

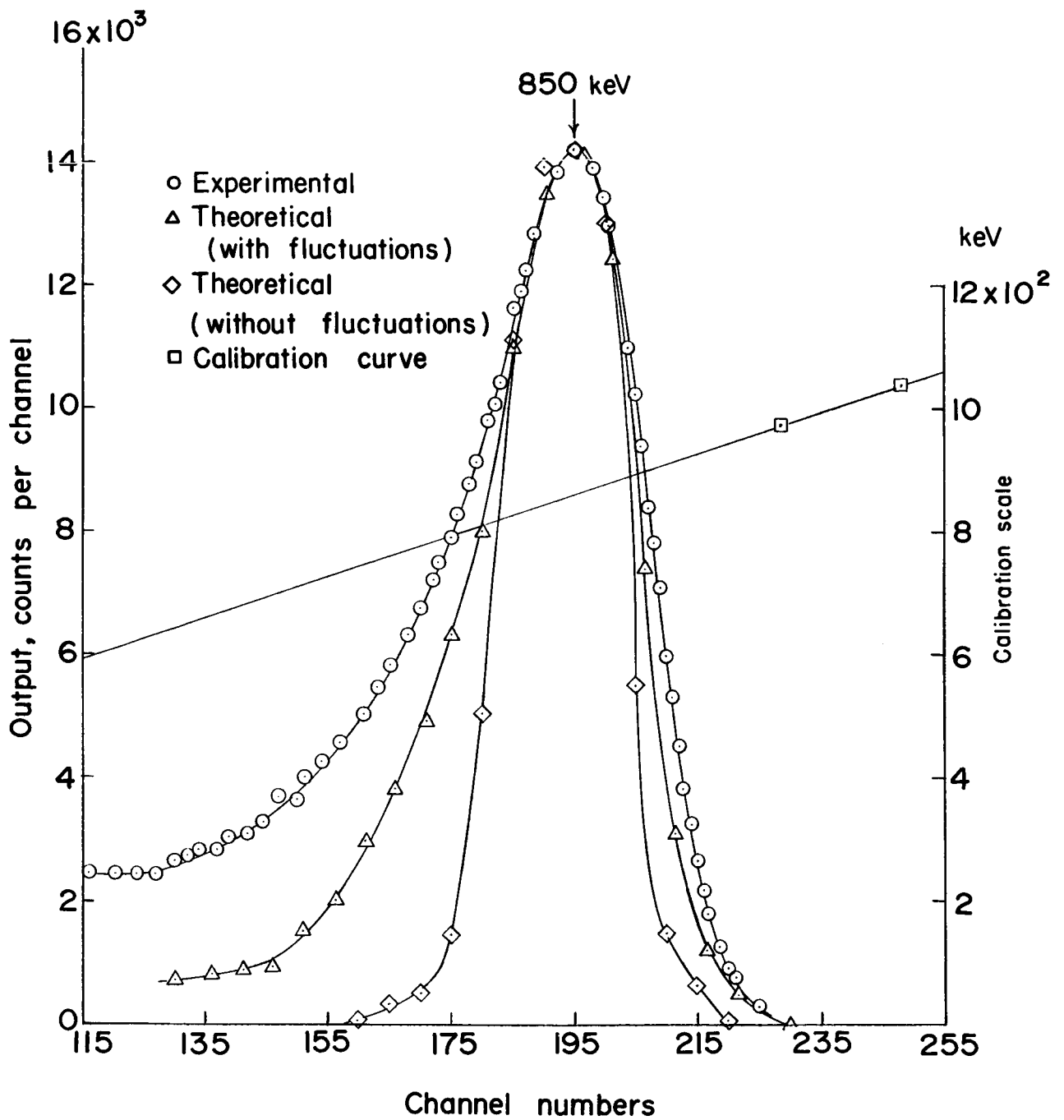


Figure 7.- Comparison between theory and experimental spectrum of 1.00-MeV electrons transmitted through 0.5-mm-thick silicon target at 30° .

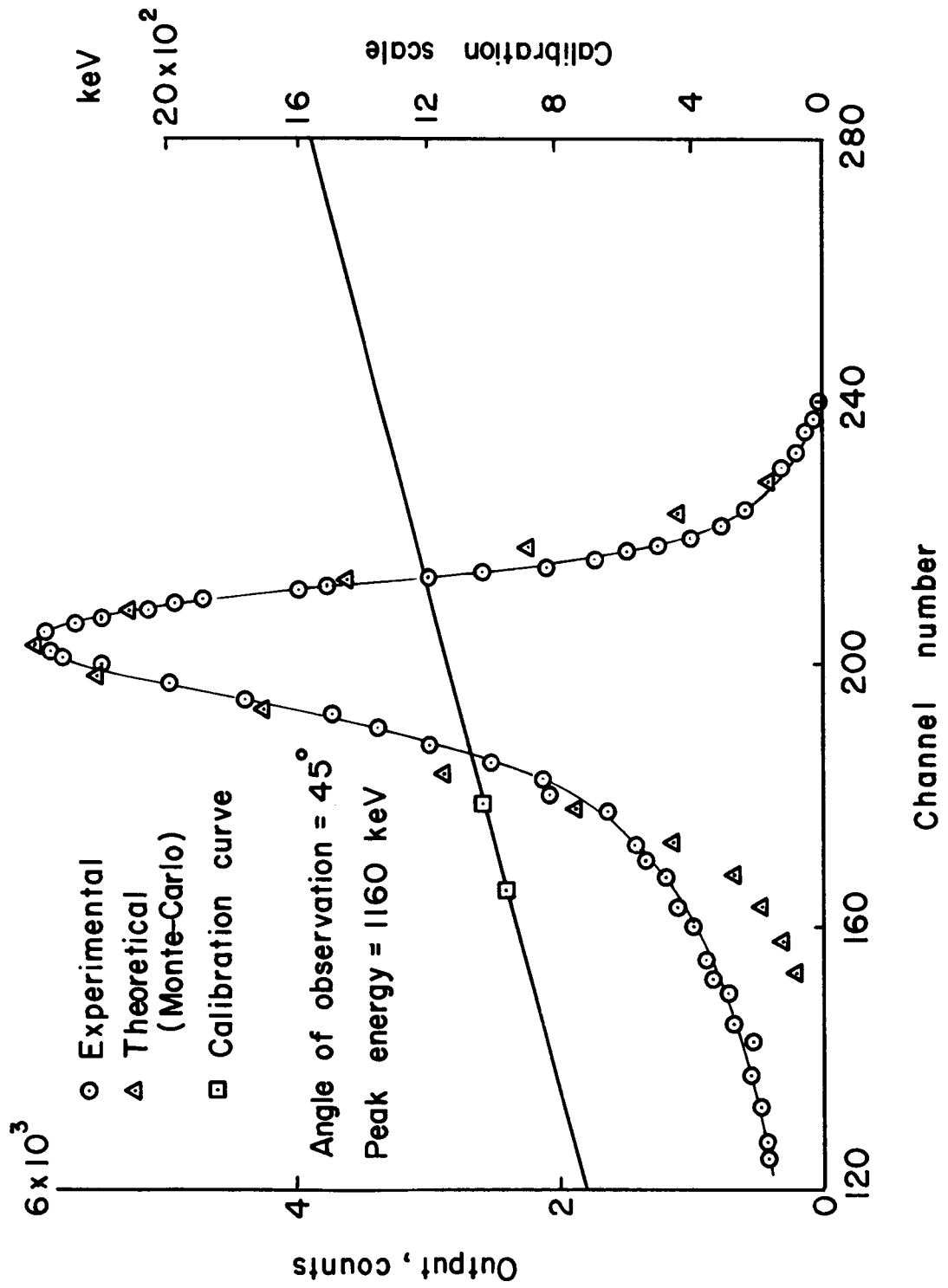


Figure 8.- Comparison between theory and experimental spectrum of 1.50-MeV electrons transmitted through 0.78-mm-thick silicon target at 45° .

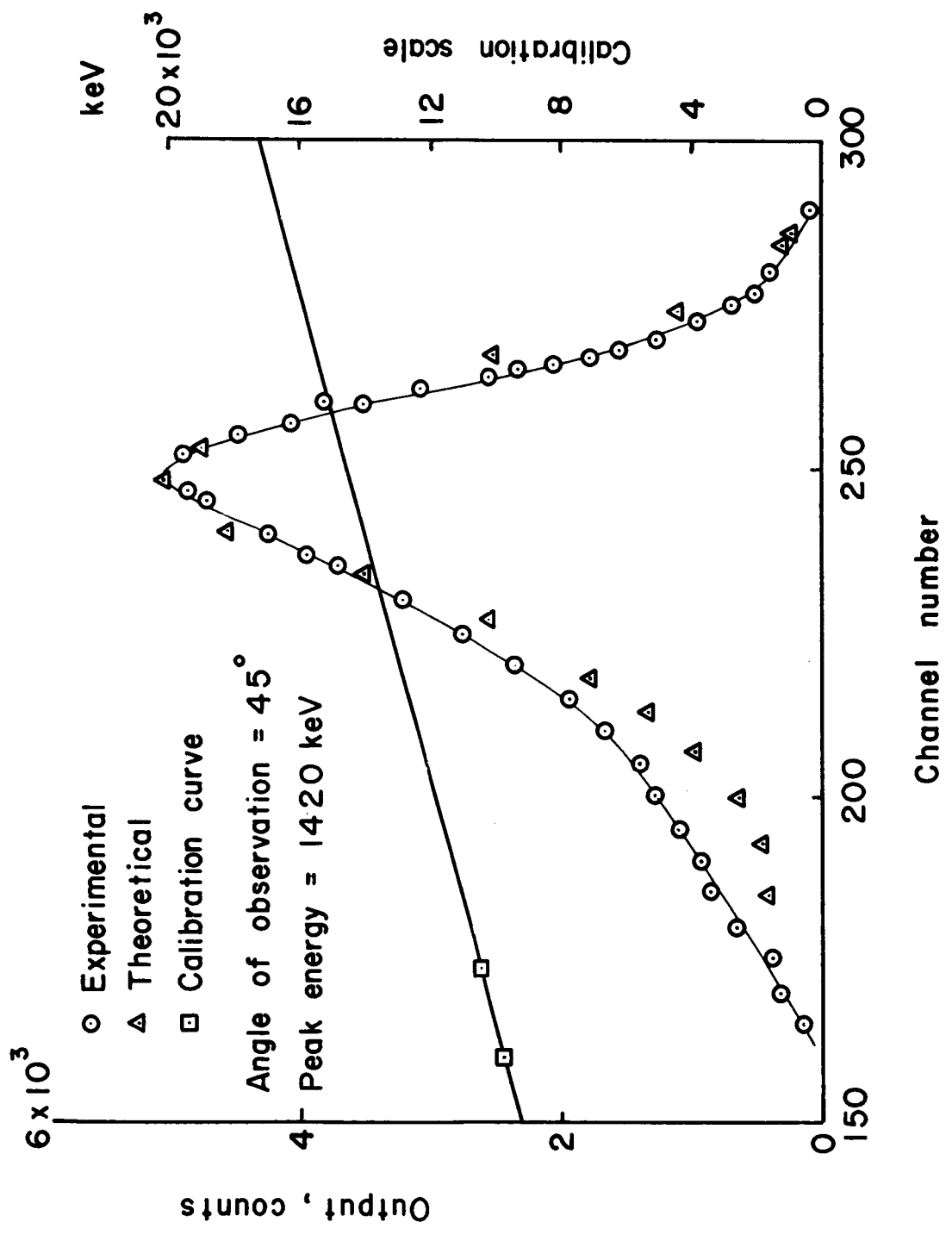


Figure 9.- Comparison between theory and experimental spectrum of 2.00-MeV electrons transmitted through 1.27-mm-thick silicon target at 45°.

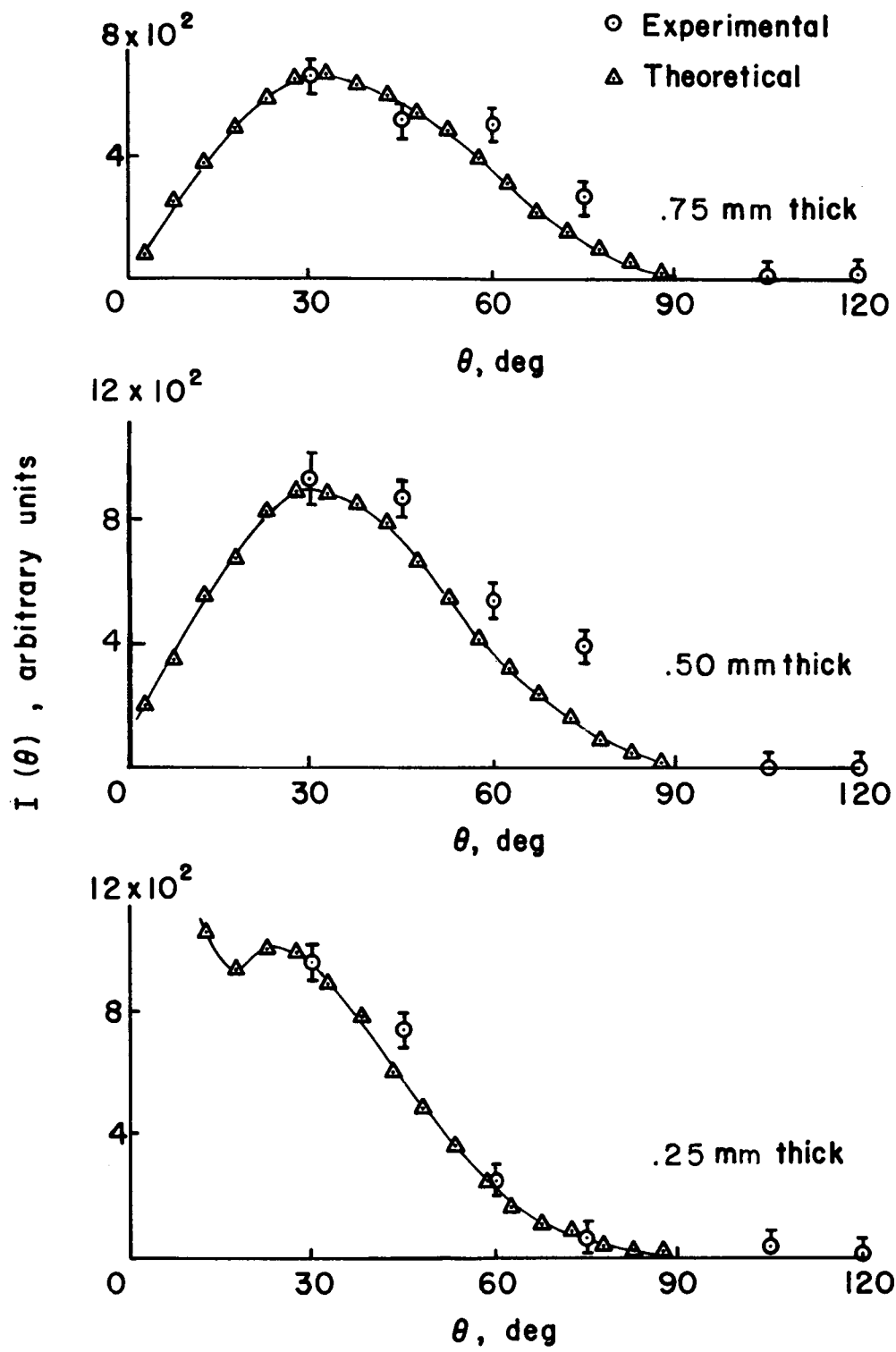


Figure 10.- Comparison between theoretical and experimental angular distributions of transmitted electrons for a number of target thicknesses at 1.00 MeV.

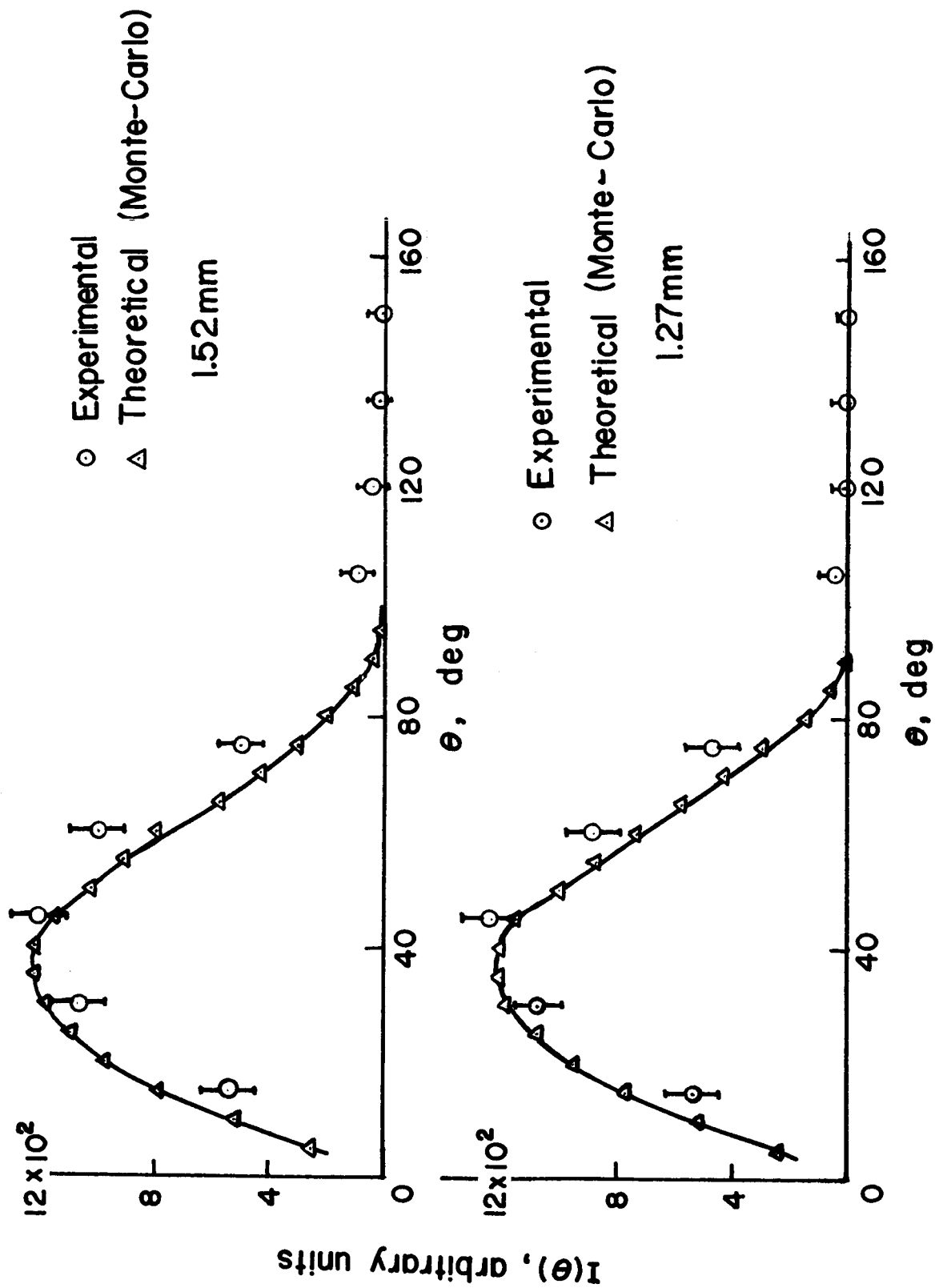


Figure 11.- Comparison between theoretical and experimental angular distributions of transmitted electrons for two different target thicknesses at 1.50 MeV.

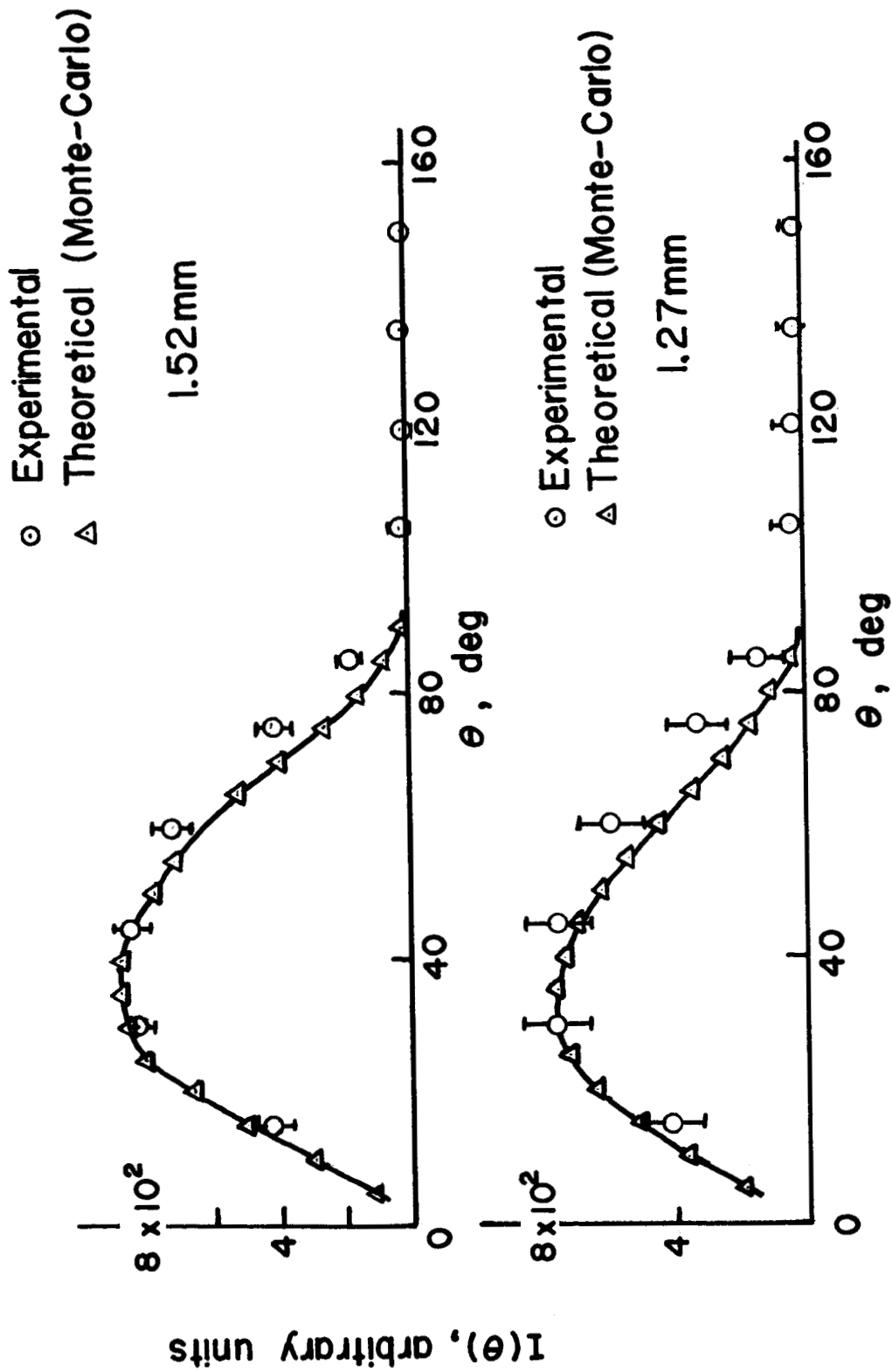


Figure 12.- Comparison between theoretical and experimental angular distributions of transmitted electrons for two different target thicknesses at 2.00 MeV.

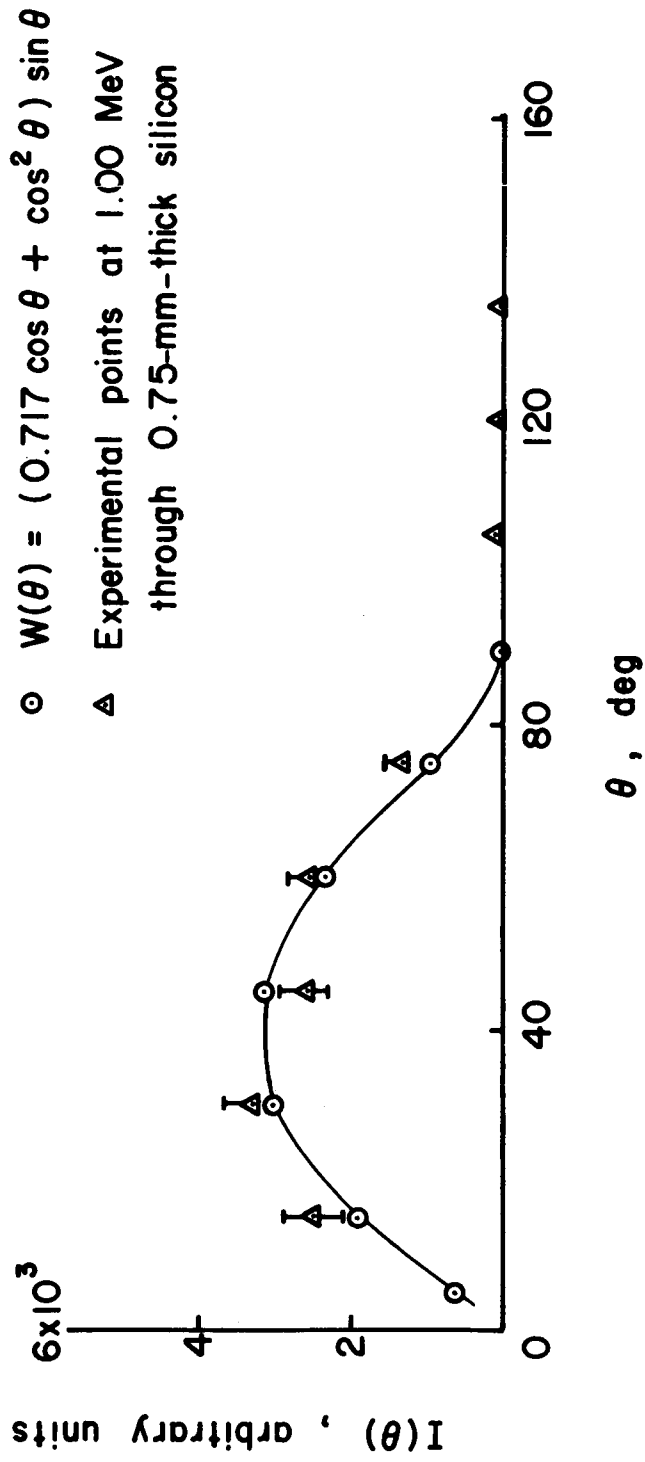


Figure 13.- Comparison between experimental angular distribution of 1.00-MeV electrons transmitted through 0.75-mm-thick silicon and a distribution function of the form $W(\theta) = (a \cos \theta + b \cos^2 \theta) \sin \theta$.

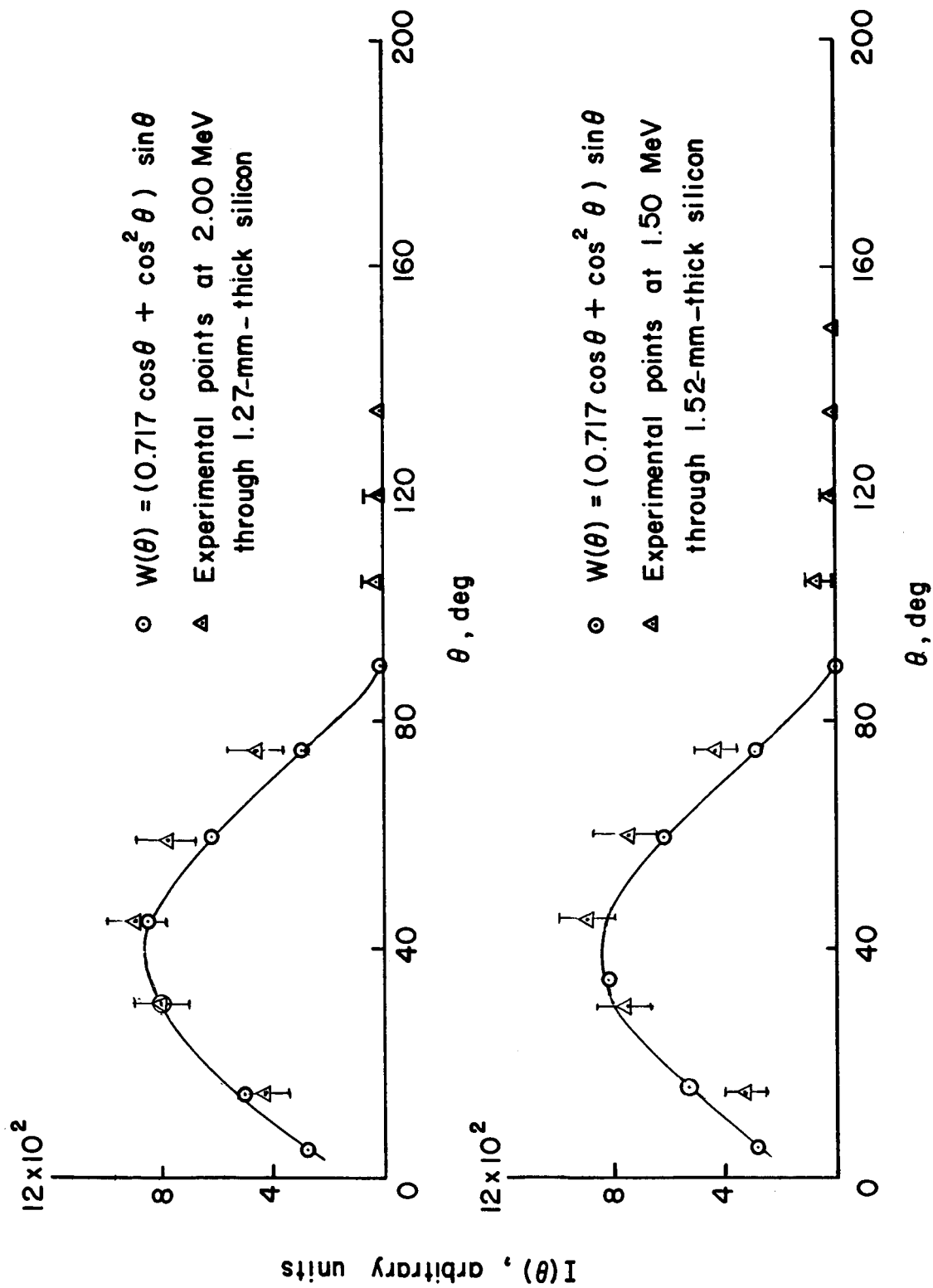


Figure 14.- Comparison of experimental angular distribution at 1.50 MeV and 2.00 MeV and a distribution function of the form $W(\theta) = (a \cos \theta + b \cos^2 \theta) \sin \theta$.

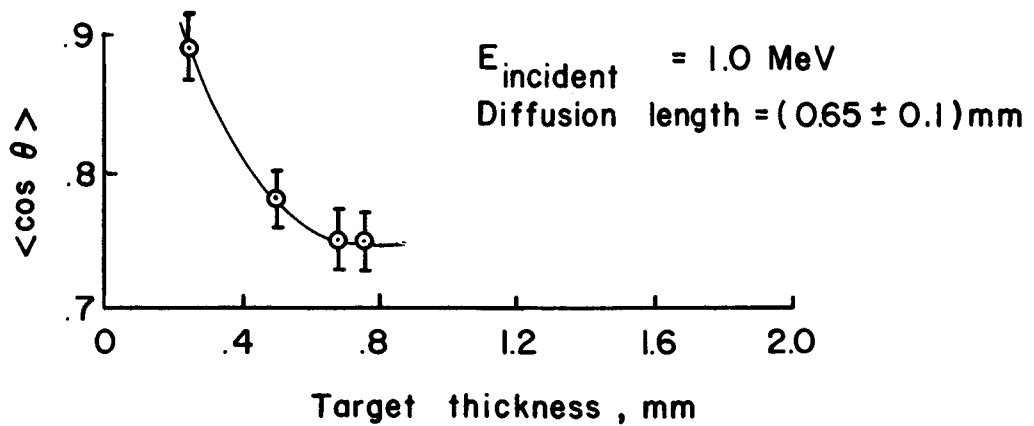
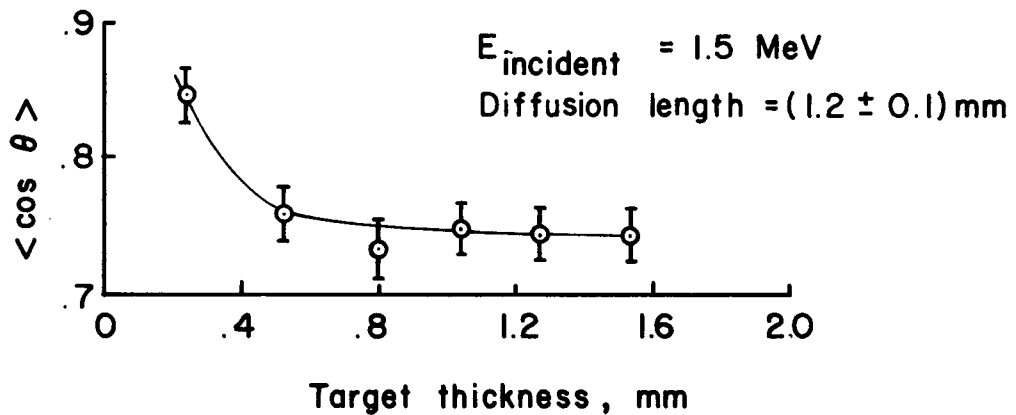
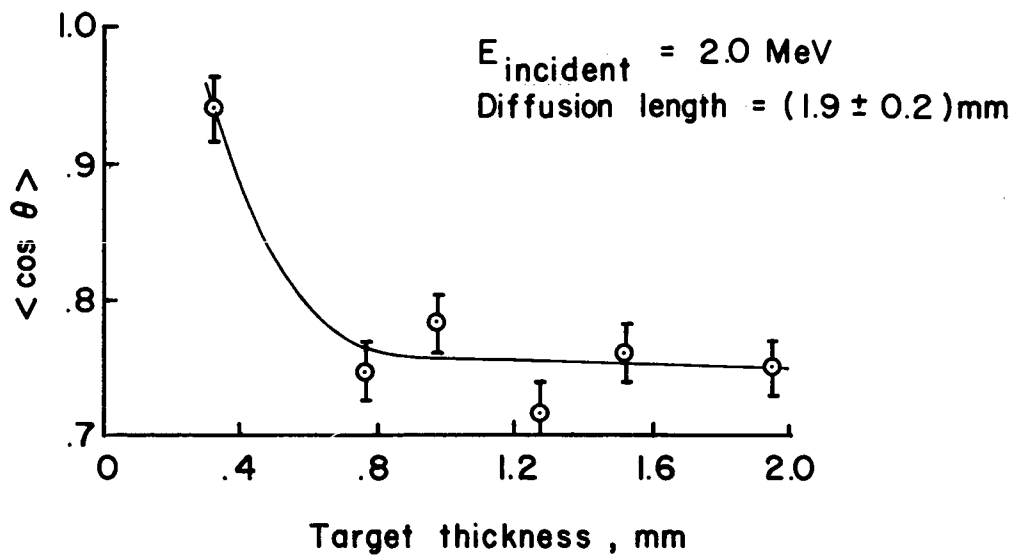


Figure 15.- Graph of average cosine θ , $\langle \cos \theta \rangle$, as a function of target thickness at three energies.